Biochemical Characterization of the RNase II Family of Exoribonucleases from the Human Pathogens *Salmonella typhimurium* and *Streptococcus pneumoniae*[†]

Susana Domingues,[‡] Rute G. Matos,[‡] Filipa P. Reis,[‡] Arsénio M. Fialho,[§] Ana Barbas,[‡] and Cecília M. Arraiano*[,‡]

[‡]*Instituto de Tecnologia Química e Biológica/Universidade Nova de Lisboa, Apartado 127, 2781-901 Oeiras, Portugal, and [§]Institute for Biotechnology and Bioengineering Centre for Biological and Chemical Engineering/Instituto Superior Técnico, Lisboa, Portugal*

ABSTRACT: Maturation, turnover, and quality control of RNA are performed by many different classes of ribonucleases. *Escherichia coli* RNase II is the prototype of the RNase II family of ribonucleases, a ubiquitous family of hydrolytic, processive $3' \rightarrow 5'$ exonucleases crucial in RNA metabolism. RNase R is a member of this family that is modulated in response to stress and has been implicated in virulence. In this work, RNase II-like proteins were characterized in the human pathogens *Salmonella typhimurium* and *Streptococcus pneumoniae*. By sequence analysis, only one member of the RNase II family was identified in *S. pneumoniae*, while both RNase II and RNase R were found in *Sa. typhimurium*. These enzymes were cloned, expressed, purified, and characterized with regard to their biochemical features and modular architecture. The specificity of substrates and the final products generated by the enzymes were clearly demonstrated. *Sa. typhimurium* RNase II and RNase R behaved essentially as their respective *E. coli* counterparts. We have shown that the only hydrolytic RNase found in *S. pneumoniae* was able to degrade structured RNAs as is the case with *E. coli* RNase R. Our results further showed that there are differences with regard to the activity and ability to bind RNA from enzymes belonging to two distinct pneumococcal strains, and this may be related to a single amino acid substitution in the catalytic domain. Since ribonucleases have not been previously characterized in *S. pneumoniae* or *Sa. typhimurium*, this work provides an important first step in the understanding of post-transcriptional control in these pathogens.

RNA metabolism plays an essential role in the control of gene expression, and several distinct ribonucleases are involved in the degradation, processing, turnover, and quality control of RNA. *Escherichia coli* RNase II and RNase R are representatives of the RNase II family of exoribonucleases, a widespread class of enzymes that have a key function in RNA metabolism and are present in prokaryotes and eukaryotes (*1−3*). *E. coli* RNase II and RNase R exhibit similar catalytic and structural properties: they both degrade RNA hydrolytically in the $3' \rightarrow 5'$ direction in a processive and sequence-independent manner. However, while RNase R is capable of degrading highly structured RNA, the RNase II activity is impaired by the presence of secondary structures (reviewed in ref *3*).

E. coli RNase II, a monomer of approximately 73 kDa encoded by the *rnb* gene, is the prototype of this family. In this bacterium, RNase II is the major hydrolytic enzyme (*4*). However, because of its strong affinity for the homopolymer poly(A), it can rapidly degrade some polyadenylated stretches necessary for degradation by other exoribonucleases, and paradoxically, it can act as a protector of full-length RNAs (*5, 6*). The enzyme is tightly regulated at the transcriptional and post-transcriptional levels, and its amount changes with growth conditions (*7, 8*).

Determination of the 3D[1] structure of *E. coli* RNase II showed that RNase II consists of four domains: two N-terminal cold shock domains (CSD1 and CSD2), one central RNB catalytic domain, and one C-terminal S1 domain (*9, 10*) (Figure 1). The biochemical and structural data allowed an understanding of the RNA degradation mechanism of this family of enzymes (*9*).

RNase R is an ~92 kDa protein encoded by the *rnr* gene and shares an identical domain organization and three-dimensional arrangement with RNase II (*11*). RNase R was initially described as a secondary exoribonuclease only responsible for the residual hydrolytic activity in *E. coli*. However, orthologues of RNase R are found in most bacteria, and recent studies have demonstrated that, in fact, this enzyme is implicated in the processing and degradation of different types of RNA, such as tRNA, rRNA, mRNA, and small RNAs (sRNA) (*12−14*). RNase R is also involved in RNA quality control, being responsible for the degradation of defective tRNA as well as the elimination of aberrant rRNA (*14−16*). The ability of RNase R to act on highly structured RNA molecules, like the small RNAs, leads to important physiological consequences. It has been reported that the correct maturation of *tm*RNA, a small RNA involved in the quality control of proteins, requires the action of this protein (*13*). All these features indicate a more specific role of RNase R in RNA metabolism. Moreover, RNase R has been shown to be

---

[1]Abbreviations: CSD, cold shock domain; RNB, RNase II catalytic domain; Amp, ampicillin; Tet, tetracycline; LB, Luria Broth; IPTG, isopropyl β-D-thiogalactoside; DTT, dithiothreitol; PMSF, phenylmethanesulfonyl fluoride, EDTA, ethylenediaminetetraacetic acid; NCBI, National Center for Biotechnology Information; HTH, helix−turn−helix; 3D, three-dimensional.
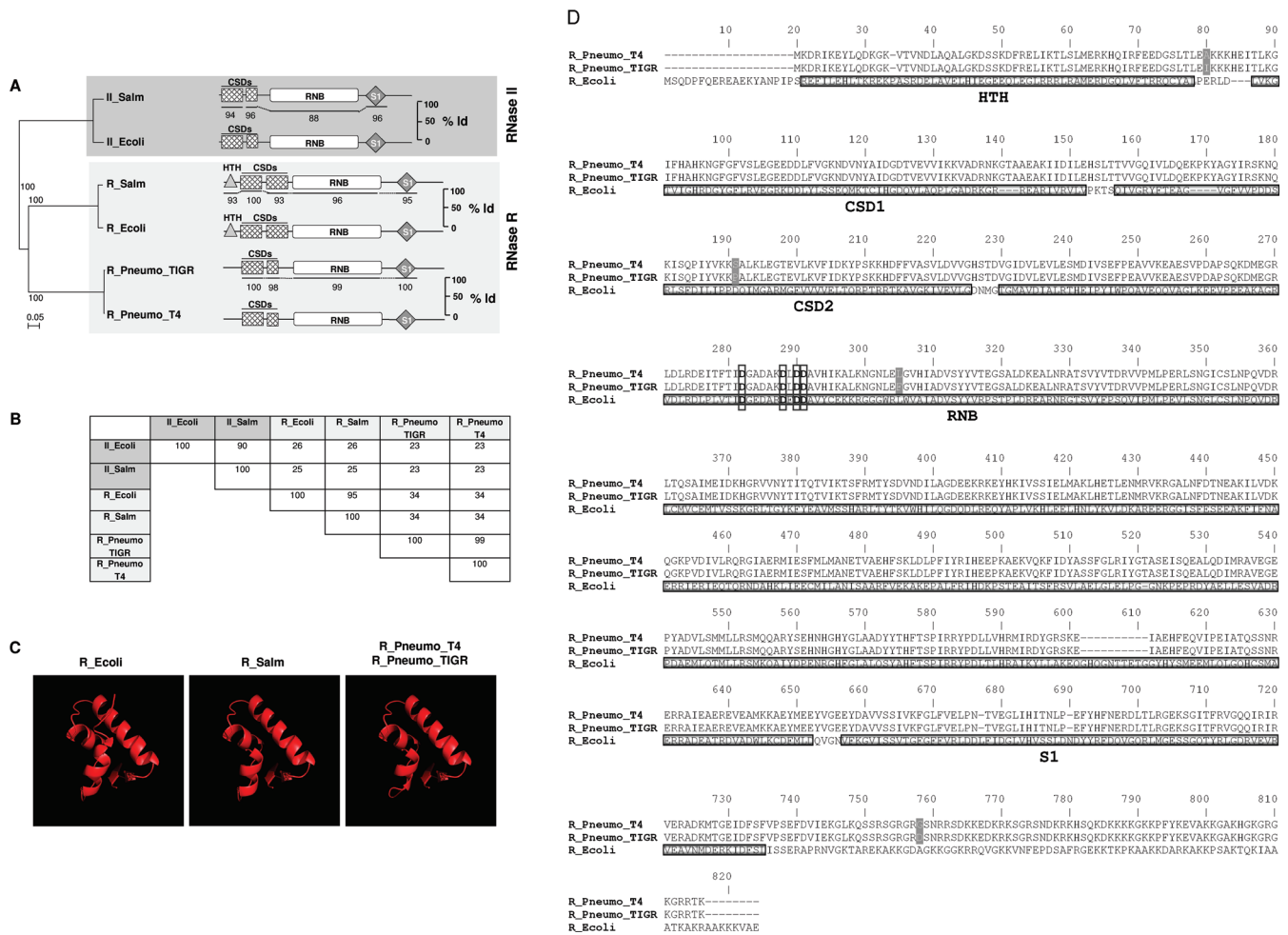
FIGURE 1: Bioinformatic analysis of proteins from the RNase II family. (A) Phylogenetic tree of the six hydrolytic enzymes, organized in two distinct groups. One group includes RNase II-like proteins (II_Ecoli and II_Salm) and the other group RNase R-like proteins (R_Ecoli R_Salm, R_Pneumo_TIGR, and R_Pneumo_T4). The values adjacent to a node indicate the percentage of 500 bootstrap trees that contain the node. The RNase R group has two branches differentiating *Salmonella typhimurium* and *E. coli* RNase R from those of *Streptococcus pneumoniae*. A schematic representation of the modular architecture of each protein produced using Pfam is shown. All the enzymes present two cold shock domains (CSD) at the N-terminus, S1 at the carboxy end and the RNB catalytic domain spanning the middle region of the proteins. An additional helix−turn−helix (HTH) motif was found in the N-terminal end of R_Ecoli and R-Salm. The amino acid identity between the domains of the enzymes of each group is also indicated. (B) Total amino acid identity among the six members of the RNase II family of exoribonucleases being studied. (C) Homology-based 3D models of the N-terminal spanning residues of the RNase R-like enzymes: R_Ecoli (amino acids 18−78), R_salm (amino acids 23−78), and R_Pneumo_T4 and R_Pneumo_TIGR (amino acids 4−58). Because of the perfect homology between R_Pneumo_T4 and R_Pneumo_TIGR in this region, only one model is shown. (D) Sequence alignment of R_Pneumo_T4, R_Pneumo_TIGR, and R_Ecoli. The alignment was prepared with ClustalW (*38*). The domains identified in R_Ecoli (HTH, CSD1, CSD2, RNB, and S1) are denoted. The four different amino acids between R_Pneumo_T4 and R_Pneumo_TIGR are highlighted in gray. The aspartate residues proposed to compose the active site are boxed (*11*).

modulated in response to different stress conditions (*12, 13, 17−21*). Previous studies have shown that RNase R is a cold shock protein, and other stress conditions were also able to induce RNase R (*13*). RNase R protein levels were shown to increase in the stationary phase (*7, 12, 22*).

Since the infection process exposes pathogens to numerous stress conditions (e.g., temperature shifts, pH changes, and nutritional deprivation), adaptation of bacteria to stress is a crucial step in the virulence process. Not surprisingly, RNase R has been involved in the modulation of the expression of virulence in a number of pathogenic organisms such as *Aeromonas hydrophyla*, *Shigella flexneri*, *Burkholderia* spp., and *Helicobacter pylori* (*20, 23−25*). In *Legionella pneumophila*, an opportunistic pathogen of human macrophages that can cause a severe and mortal disease, RNase R is the only hydrolytic exoribonuclease, and its loss has a significant impact in *L. pneumophila* growth and viability at low temperatures (*18*). In *Mycoplasma genitalium*, a human pathogen

linked to urethritis and other sexually transmitted diseases, RNase R has been the only exoribonuclease identified, being an essential enzyme in this organism (*26−28*).

Streptococcus pneumoniae is a human pathogen that is the major cause of pneumonia, septicemia, meningitis, and otitis. It is also one of the principal causes of septicemia in HIV-infected individuals. Collectively, these diseases result in millions of deaths worldwide each year. The currently available vaccine is only partially effective, and multiple drug-resistant strains of this pathogen have emerged in recent years (*29*). For this reason, great effort to understand the mechanisms of pathogenesis is being spent to identify new targets for vaccines and novel drugs.

Salmonella infections are a serious medical and veterinary problem worldwide. Meat and eggs contaminated with *Salmonella enterica* sv. *typhimurium* (*Salmonella typhimurium*) are common fonts of acute gastroenteritis in humans (*15*). Salmonellosis constitutes a health problem, especially for fecal

contamination of water resources, and new strategies for prevention and control are necessary. The understanding of *Salmonella* cellular control mechanisms may lead to identification of novel targets for therapeutic intervention.

Since it has been shown that exoribonucleases are involved in virulence and practically nothing is known about RNases in *S. pneumoniae* or *Sa. typhimurium*, the characterization of the biochemical properties of the exoribonucleases in these organisms may be useful for further understanding the virulence mechanisms. To achieve this purpose, we performed a search of the available genomic sequences of *Sa. typhimurium* and *S. pneumoniae*. Two homologues of the RNase II family of proteins were indentified in *Sa. typhimurium*, while only one member of this family was found in *S. pneumoniae* (Figure 1). Both hydrolytic enzymes from *Sa. typhimurium* and the RNase R-like enzyme from two different *S. pneumoniae* strains were cloned, overexpressed, purified, and characterized with regard to their RNA binding ability and exonucleolytic activity. The results clearly show the specificity of substrates and the end products generated by each enzyme. In agreement with the in silico analysis, *Sa. typhimurium* contains both hydrolytic enzymes, RNase II and RNase R, while the only enzyme present in *S. pneumoniae* behaves like RNase R. Interestingly, *Sa. typhimurium* RNase II can approach the double-stranded region more closely than the *E. coli* homologue. Besides RNase R, *S. pneumoniae* also contains a PNPase-like exoribonuclease. To the best of our knowledge, this is the first time that an RNase R from a Gram-positive bacterium with this genetic background has been studied. Our results further show that a single amino acid substitution may be responsible for the different biochemical properties exhibited by the two pneumococcal RNase R-like proteins studied.

EXPERIMENTAL PROCEDURES

Materials. Restriction enzymes, T4 DNA ligase, and T4 polynucleotide kinase were purchased from New England Biolabs, and Pfu DNA polymerase was from Fermentas. Unlabeled oligonucleotide primers were synthesized by STAB Vida. The sequence of the *rnr* gene from *S. pneumoniae* strain T4, a derivative of *S. pneumoniae* R6 (*30*), was determined on double-stranded DNA using the appropriate primers. This sequence was deposited in GenBank (accession number FJ999997). The sequence of the *rnr* gene from *S. pneumoniae* TIGR4 was confirmed on double-stranded DNA with the appropriate primers.

Bacterial Strains and Growth Conditions. The following *E. coli* strains were used: DH5α [fhuA2 Δ(argF-lacZ)U169 phoA glnV44 Φ80 Δ(lacZ)M15 gyrA96 recA1 relA1 endA1 thi-1 hsdR17 (*31*)] and NovaBlue (endA1 hsdR17 supE44 thi-1 recA1 gyrA86 relA1 lac [F′ proA⁺B⁺ lacI�q lacZΔM15::Tn10]) (Novagene) for cloning experiments and BL21(DE3) [F⁻ r_B^- m_B^- gal ompT (int::P$_{lacUV5}$ T7 gen1 imm21 nin5) (*32*)] for expression of the enzymes. *E. coli* BL21(DE3) strains expressing *E. coli* RNase II and *E. coli* RNase R have been previously described (*33, 34*).

E. coli was cultivated in Luria Broth (LB) medium at 37 °C, except when specified differently. When required, this medium was supplemented with 200 μg/mL ampicillin (Amp), 15 μg/mL tetracycline (Tet), and 0.4% glucose.

Construction of Recombinant Proteins. All genes encoding the proteins in this study were cloned into the pET-15b vector

Table 1: Primer Sequences Used in This Study[a]

primer	sequence (5′–3′)
smd005	ggaattccatATGTTTCAGGACAACCCGC
smd006	cgcggatccGTGGTTACGCTGCCGGTCGG
smd007	ggaatctcgagATGTCACAAGATCCTTTCC
smd008	ccggaattcGCTCACTCTGCCGCTTTTTTC
rnrNde	ggaattccatATGAAAGATAGAATAAAAGAATATTTAC
rnrBam	cgcggatccTACGATTGTATAGTCGTGGCGTGCC

[a]Lowercase letters indicate restriction sites.

(Novagen) under the control of the φ10 T7 promoter, allowing the expression of His$_6$-tagged fusion proteins. The primers used for the construction of the recombinant proteins are listed in Table 1. *Pfu* DNA polymerase (Fermentas) was used in PCRs (polymerase chain reactions). *Sa. typhimurium* SL1344 *rnr* (also known as *vacB*) and *rnb* genes were amplified from genomic DNA supplied by S. Viegas (*35*) using primers smd007/smd008 and smd005/smd006, respectively. The genes encoding the hydrolytic RNase from *S. pneumoniae* T4 and TIGR4 strains were amplified from genomic DNA kindly supplied by P. Lopez (CIB-CSIC, Madrid, Spain) using primers rnrNde and rnrBam. The amplified fragments were cloned into the NdeI/BamHI site of pET-15b except the *rnb* PCR product, which was cloned into the EcoRI/XhoI site of the same plasmid. *Sa. typhimurium* genes were first cloned into *E. coli* DH5α, while the plasmid containing the *rnr* genes derived from *S. pneumoniae* was transformed into *E. coli* Novablue and selected in LB medium supplemented with Tet and glucose, besides Amp. The plasmids were subsequently transformed into *E. coli* strain BL21(DE3) (Novagen) to allow the expression of the recombinant proteins. As a negative control used in all the following experiments, pET-15b (without insert) was also transformed into BL21(DE3). All constructs were confirmed by DNA sequencing at STAB Vida (Oeiras, Portugal).

Overexpression and Purification of RNase II-like Proteins. Recombinant proteins were expressed and purified following the strategy previously described for the purification of *E. coli* RNase II and RNase R (*33, 34, 36*). Briefly, *E. coli* BL21(DE3) containing the recombinant plasmid of interest was grown at 37 °C in 200 mL of LB medium supplemented with 200 μg/mL Amp to an optical density at 600 nm (OD$_{600}$) of ≈0.5. Protein expression was then induced by addition of 1 mM IPTG for 3 h at 37 °C. Cells were harvested by centrifugation and stored at −80 °C.

Purification of all proteins was performed by histidine affinity chromatography using HisTrap Chelating HP columns (GE Healthcare) and an AKTA HPLC system (GE Healthcare) following the protocol previously described (*33, 36*). Briefly, frozen cells were thawed and resuspended on 6 mL of buffer A [20 mM Tris-HCl, 0.5 M NaCl, 1 mM DTT, and 5 mM imidazole (pH 8)]. Cell suspensions were lysed using a French press at 9000 psi in the presence of 0.1 mM PMSF. The crude extracts were treated with Benzonase (Sigma) to degrade the nucleic acids and clarified by a 30 min centrifugation at 10000*g*. The clarified extracts were then loaded into a HisTrap Chelating Sepharose 1 mL column equilibrated in buffer A. Protein elution was achieved with a continuous imidazole gradient (from 20 to 500 mM) in buffer A.

Eluted protein was buffer exchanged with buffer C [20 mM Tris-HCl, 250 mM NaCl, and 1 mM DTT (pH 8)] and concentrated by centrifugation at 4 °C with Amicon Ultra Centrifugal

Filter Devices (Millipore) with a molecular mass cutoff of 50 kDa. Protein concentrations were determined by spectrophotometry using a NanoDrop 1000 instrument (Alfagene), and 50% (v/v) glycerol was added to the final fractions prior to storage at −20 °C. The purity of the enzymes was analyzed by sodium dodecyl sulfate−polyacrylamide gel electrophoresis (SDS−PAGE) and revealed ∼90% homogeneity (supplementary data).

The strategy described above was followed for the control strain [*E. coli* BL21(DE3) containing pET-15b without an insert]. The obtained protein extract was used as a negative control in all the experiments performed with the recombinant proteins.

Western Immunoblotting. His-tagged recombinant proteins were analyzed by Western immunoblotting. For this purpose, purified proteins were separated by SDS−PAGE and transferred to a nitrocellulose membrane (Hybond ECL, GE Healthcare) by electroblotting using the Trans-Blot SD semidry electrophoretic system (Bio-Rad). Membranes were probed with a 1:3000 dilution of anti-His antibodies (GE Healthcare). ECL anti-mouse IgG-conjugated horseradish peroxidase (from sheep) was used as the secondary reagent in a 1:5000 dilution. Immunodetection was conducted via a chemiluminescence reaction using Amersham ECL Western Blotting Detection Reagents (GE Healthcare).

Activity Assays. Exoribonucleolytic activity was assayed using oligoribonucleotides as substrates. The 30-mer (5′-CCC-GACACCAACCACUAAAAAAAAAAAAAAA-3′) and 35-mer poly(A) oligoribonucleotides were labeled at their 5′-ends with $[\gamma\text{-}^{32}\text{P}]\text{ATP}$ with T4 polynucleotide kinase. The labeled 30-mer ribonucleotide was hybridized to the complementary 16-mer deoxyribonucleotide (5′-AGTGGTTGGTGTCGGG-3′), thus yielding the corresponding double-stranded substrates (16−30ds) (*36*). The hybridization was performed in a 1:1 (molar) ratio in the Tris component of the activity buffer by incubation for 5 min at 68 °C followed by 45 min at room temperature. The exoribonucleolytic reactions were performed in a final volume of 12.5 μL containing the same activity buffer as previously described (*37*). In all cases, 30 nM single-stranded (nonhybridized) or double-stranded (hybridized) oligonucleotide substrates were used, and the amount of each enzyme was adjusted to achieve linear kinetics. Reactions were started by the addition of the enzyme and mixtures incubated at 37 °C. Samples were withdrawn at the times indicated in the figures, and the reaction was stopped via addition of formamide-containing dye supplemented with 10 mM EDTA. Reaction products were resolved in a 20% polyacrylamide/7 M urea gel and analyzed by autoradiography. The exoribonucleolytic activity of the enzymes was determined by measuring and quantifying the disappearance of the substrate in several distinct experiments, and each value obtained represents the mean of three independent assays. The relative activity for all proteins was standardized for a 1 min reaction per 1 nmol of protein. The specific activity of each enzyme is given as picomoles of substrate oligoribonucleotide consumed per minute per nanomole of protein at 37 °C. For quantification, the amount of purified enzyme used was selected to ensure that less than 25% of the substrate was degraded. The results obtained are listed in Table 2.

Surface Plasmon Resonance Analysis (*Biacore*). Biacore SA chips were obtained from Biacore Inc. (GE Healthcare). The flow cells of the SA streptavidin sensor chip were coated with a low concentration of the RNA substrate. On flow cell 1, no substrate was added so this cell could be used as the control blank cell. On flow cell 2, a 5′-biotinylated 25-nucleotide RNA oligomer (5′-CCCGACACCAACCACUAAAAAAAAAA-3′) was added

to allow the study of the interaction of the protein with a single-stranded RNA molecule. On flow cell 3, a 5′-biotinylated 30-nucleotide poly(A) oligomer was added to allow the study of the interaction of the protein with a single-stranded RNA molecule composed only of adenosines. The target RNA substrates were captured on the respective flow cells by 20 μL triple injections of a 500 nM solution of the target RNA in 1 M NaCl at a flow rate of 10 μL/min, as described in previous reports (*11*, *38*). The biosensor assay was conducted at 4 °C in a buffer composed of 20 mM Tris-HCl (pH 8), 100 mM KCl, 1 mM DTT, and 25 mM EDTA. The proteins were injected over flow cells 1−3 for 2 min at concentrations of 10, 20, 30, 40, and 50 nM using a flow rate of 20 μL/min. All experiments included triple injections of each protein concentration to determine the reproducibility of the signal and control injections to assess the stability of the RNA surface during the experiment. Bound protein was removed with a 60 s wash with 2 M NaCl, which did not damage the substrate surface. Data from flow cell 1 were used to correct for refractive index changes and nonspecific binding. To ensure that during SPR analysis the exoribonucleolytic activity of the proteins studied was completely blocked, we conducted these experiments in a buffer with a 2.5-fold higher concentration of EDTA [25 mM instead of the usual 10 mM used in RNA binding assays (*33*)]. Under these conditions, we can be sure that EDTA saturation was obtained and that there is no degradation of the RNA substrate by the enzymes. Rate constants and equilibrium constants were calculated using BIA EVALUATION version 3.0, according to the 1:1 Langmuir binding fitting model. The dissociation constants (K_D) obtained are listed in Table 3.

Multiple-Sequence Alignment, Phylogenetic Tree Construction, Domain Architecture Analysis, and 3D Homology Modeling. Sequence similarity searches were performed using BLAST 2.0 at the NCBI. Multiple-sequence alignments of the six-RNase II family of exoribonucleases were conducted using CLUSTAL X 1.83 with default parameters (*39*). The resulting alignment was used to calculate the distance matrix by the Tree-puzzle method (*40*). The phylogenetic tree was constructed by the Neighbor-Joining method (*41*) and supported by 500 bootstrap steps (*42*). The amino acid sequences of the exoribonucleases under study were searched in the Pfam A (http://pfam.sanger.ac.uk/) (*43*) database for the annotation of domains and their arrangements. The 3D models for the proteins in study were determined using standard homology modeling methods based on the multiple-sequence alignment of the family members. The model structures were built using the Phyre webserver [http://www.sbg.bio.ic.ac.uk/phyre (*44*)]. 3D models for the RNase II family members were based on the crystal structures of wild-type RNase II and the RNase II D209N mutant complexed with a 13-nucleotide poly(A) RNA [Protein Data Bank (PDB) entries 2IX1 and 2IX0 (*9*)]. Because of the lack of the N-terminal HTH motif in these crystal structures, the 3D models of the additional N-terminal region of RNase R-like proteins were based on the crystal structure of PDB entry 1mkm (*45*). Structure figures were generated with Pymol (*46*).

RESULTS

RNase II-like Enzymes from Salmonella and Streptococcus. RNases have been involved in the virulence mechanisms of several pathogenic organisms (*18*, *20*, *24*, *47*, *48*), and an improved understanding of the biochemical mode of action of these proteins may be important for further studies on virulence.

Table 2: Exoribonucleolytic Activities of Proteins from the RNase II Family[a]

protein	protein activity (pmol min^{-1} nmol^{-1})
II_Ecoli	299.4 ± 36.0
R_Ecoli	130.8 ± 6.3
II_Salm	87.5 ± 2.1
R_Salm	72.8 ± 7.3
R_Pneumo_T4	3.4 ± 0.03
R_Pneumo_TIGR	7.5 ± 0.02

[a]Exoribonucleolytic activity was assayed using a 35-nucleotide poly(A) chain as a substrate. Activity assays were performed in triplicate as described in Experimental Procedures. Each value represents the number of picomoles of substrate oligoribonucleotide consumed per minute per nanomole of protein.

Table 3: RNA Binding Affinities of Proteins from the RNase II Family[a]

protein	25-mer ssRNA K_D (nM)	poly(A) ssRNA K_D (nM)
pET15b	ND[b]	ND[b]
II_Ecoli	6.5 ± 0.4	1.3 ± 0.4
R_Ecoli	3.2 ± 0.4	1.2 ± 0.1
II_Salm	12.0 ± 2.0	3.7 ± 0.1
R_Salm	19.7 ± 1.6	7.0 ± 0.6
R_Pneumo_T4	16.9 ± 1.6	5.7 ± 0.7
R_Pneumo_TIGR	9.6 ± 0.6	3.3 ± 0.2

[a]The dissociation constants (K_D) were determined by surface plasmon resonance using a Biacore 2000 instrument with a 25-nucleotide RNA oligomer (5′-biotin-CCC GAC ACC AAC CAC UAA AAA AAA A-3′) and a 30-nucleotide poly(A) RNA oligomer (5′-biotin-AAA AAA AAA AAA AAA AAA AAA AAA A-3′). [b]Not detected (no binding affinity detected for this negative control).

Hence, we decided to characterize the members of the RNase II family of enzymes of *Sa. typhimurium* and *S. pneumoniae*, two clinically important human pathogens.

Results of the phylogenetic analysis of the RNase II family of enzymes of *Sa. typhimurium* and *S. pneumoniae* are shown in Figure 1. The phylogenetic tree reveals that these enzymes form two distinct groups that clearly separate the *E. coli* enzymes RNase II and RNase R. Although the enzymes share the same domain architecture, the level of sequence identity is very low between proteins from different groups (Figure 1B). Interestingly, besides the domains previously described for the RNase II family of proteins (two CSD, one RNB, and one S1), a search in the Pfam database identified a helix−turn−helix (HTH) motif in the N-terminus of the two enteric RNase R-like proteins. However, when a more thorough analysis was conducted, by recurring to homology-based 3D modeling using only the N-terminal spanning amino acids of the enzymes, the same domain was detected in both RNase R-like proteins of *S. pneumoniae* (Figure 1C). Interestingly, this motif seems to be highly conserved among RNase R-like enzymes and may assist in RNA binding. The HTH domain is found in many proteins that regulate gene expression and has been described as a major structural motif capable of binding nucleic acids (49). Although the HTH motif has typically been associated with DNA binding, it has also been reported in RNA-binding proteins (50, 51).

Both *E. coli* and *Sa. typhimurium* belong to the Enterobacteriaceae family, and as such, the presence of two hydrolytic RNases in the *Sa. typhimurium* genome is not surprising. One of the *Sa. typhimurium* proteins studied in this report is found jointly with *E. coli* RNase II, while the other is grouped together with

E. coli RNase R. When the genome of *S. pneumoniae* was analyzed, only one hydrolytic RNase could be found. This enzyme falls in the RNase R cluster together with *E. coli* and *Sa. typhimurium* RNase R (Figure 1A). Although the comparison of the protein domains shows that the level of amino acid identity is very high among the enzymes of the same group, this value decreases significantly (to < 40%) when the entire sequence of the proteins is compared (Figure 1B). Therefore, in the phylogenetic tree, *E. coli* and *Salmonella* RNase R are found together in the same cluster while the pneumococcal orthologues form an independent cluster.

This analysis indicates that *Sa. typhimurium* contains both hydrolytic enzymes, an RNase II-like and an RNase R-like enzyme, while the only enzyme present in *S. pneumoniae* is an RNase R-like form. Via comparison of the RNase R sequence of *S. pneumoniae* TIGR4 with that of *S. pneumoniae* T4, four different amino acids were detected (Figure 1D). Thus, we decided to characterize both proteins, since it could be interesting to study the biochemical mode of action of two enzymes presenting small amino acid differences. The choice of these two strains was also based on the fact that TIGR4 is highly virulent, while T4 is a nonvirulent strain.

The hydrolytic enzymes found in *Sa. typhimurium* and *S. pneumoniae* carrying an N-terminal His tag were purified by affinity chromatography and characterized in vitro and their biochemical properties compared to those of their *E. coli* homologues. The purity and homogeneity of the purified proteins were evaluated by SDS−PAGE, and all the purified proteins were immunodetected with an anti-His antibody (data not shown). Interestingly, when using *E. coli* RNase II antibodies, not only the purified *E. coli* RNase II but also, although with lower intensity, all the other enzymes of the RNase II family were detected (data not shown). The same was observed with *E. coli* RNase R specific antibodies. These data reinforce the structural resemblance between the proteins belonging to this family (9, 11).

Exoribonuclease Activity. The behavior of the purified proteins with regard to their exoribonuclease activity against different RNA substrates was studied and compared to that of the *E. coli* homologue enzymes (11, 33, 34, 52). Activity assays were performed using two RNA molecules as substrates, a single-stranded 35-mer poly(A) and a double-stranded RNA substrate, 16−30ds.

It is known that *E. coli* RNase II is able to degrade single-stranded substrates until it reaches a four-nucleotide fragment as an end product, while RNase R is able to degrade a few more nucleotides, releasing a final product of two nucleotides (34). When we analyzed the exoribonucleolytic activity of the homologous proteins from *Sa. typhimurium* and *S. pneumoniae* using a 35-nucleotide poly(A) RNA substrate, we observed that *Sa. typhimurium* RNase II (II_Salm) behaves like *E. coli* RNase II (II_Ecoli), since its final end product also contains four nucleotides, while all the other proteins behave like *E. coli* RNase R (R_Ecoli), rendering a two-nucleotide fragment as the final product (Figure 2A).

However, there are some differences with regard to the exoribonucleolytic activity. While II_Ecoli presents an activity of 299.4 ± 36.0 pmol min^{-1} nmol^{-1}, its homologue II_Salm has an activity that is ∼3.5-fold lower, 87.5 ± 2.1 pmol min^{-1} nmol^{-1} (Table 2). The variation is not so significant between the activities of R_Ecoli and R_Salm, with R_Ecoli being only 2-fold more active than its R_Salm homologue [130.8 ± 6.3 and 72.8 ± 7.3 pmol min^{-1} nmol^{-1}, respectively (Table 2)]. When the activity of

A

PolyA 5' AAA AAA AAA AAA AAA AAA AAA AAA AAA AAA 3'

B

16-30ds 5' CCC GAC ACC AAC CAC UAA AAA AAA AAA AAA 3'
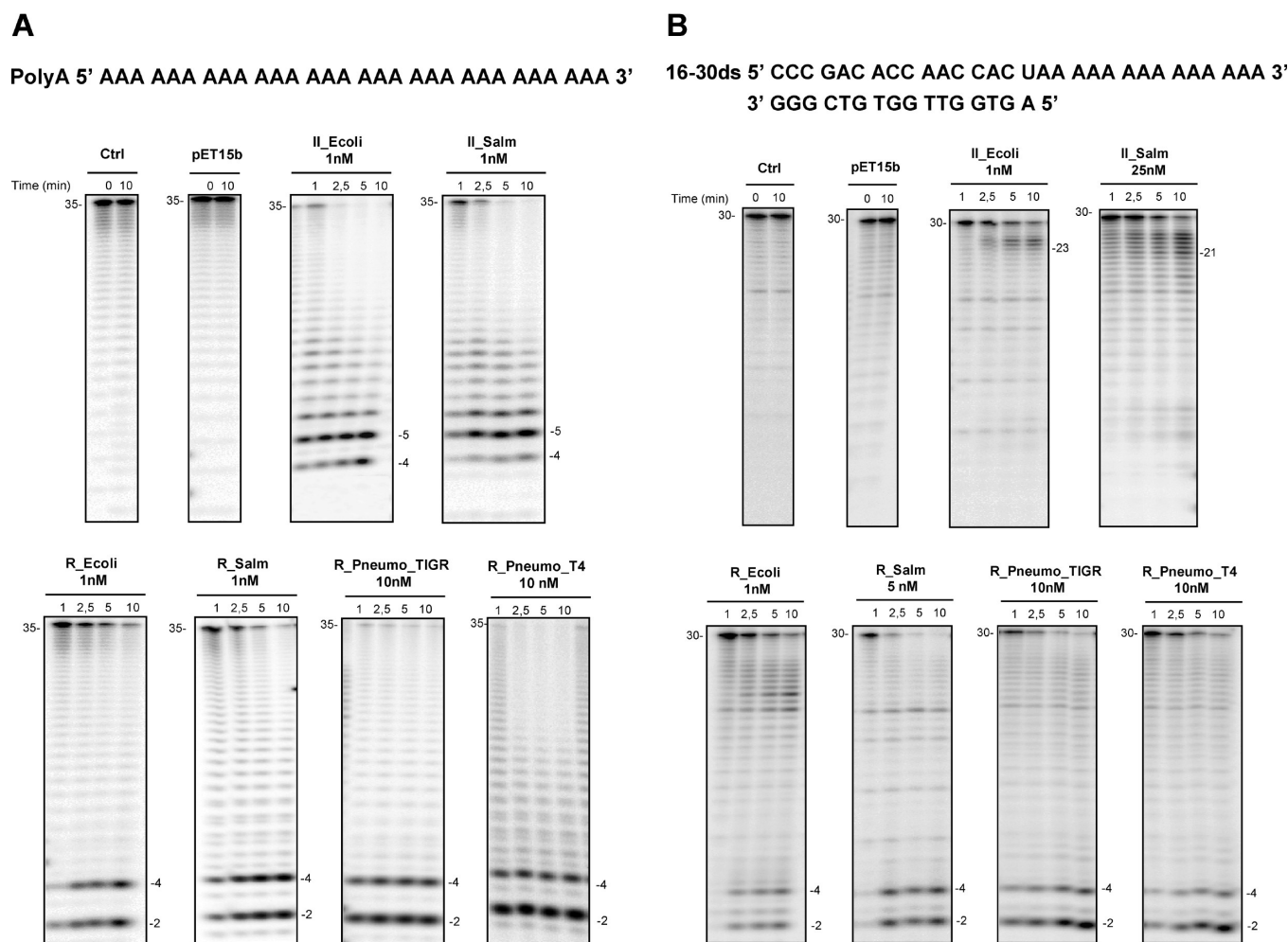**3' GGG CTG TGG TTG GTG A 5'**

FIGURE 2: Exoribonuclease activity of RNase II homologues. The quantity of enzyme used in each reaction is specified on top. Samples were taken at the indicated time points. Reaction products were analyzed in a denaturing 20% polyacrylamide gel with 7 M urea. Control reaction mixtures with no enzyme added (Ctrl) were incubated at the maximum reaction time for each protein. In all the experiments, pET15b indicates the negative control, corresponding to the addition of the protein extract obtained under the same conditions, from a strain carrying only the expression vector (pET-15b). Lengths of substrates and degradation products are indicated. (A) 30 nM 30-nucleotide poly(A) molecule used as the substrate and (B) 30 nM 16−30ds molecule used as the substrate.

the enzymes from *S. pneumoniae* (R_Pneumo_TIGR and R_Pneumo_T4) is compared, the difference is more pronounced, with R_Ecoli being 17-fold more active than R_Pneumo_TIGR and 40-fold more active than R_Pneumo_T4 (Table 2).

Besides the divergence with regard to the final end product of the reaction, another distinguishing feature between RNase II and RNase R resides in their ability to degrade structured RNA. While RNase R is capable of overcoming the secondary structures, RNase II stalls seven to nine nucleotides before it reaches the double-stranded region (*9, 33*). Thus, to test the ability of these enzymes to digest through secondary structures, we performed activity assays using a double-stranded substrate with an additional 14-nucleotide single-stranded extension at the 3'-end (16−30ds). Previous results have shown that *E. coli* RNase II is able to catalyze the rapid shortening of the 3'-single-stranded portion of this 16−30ds substrate, generating 23−25-nucleotide fragments as final products (*33*). II_Salm, as expected, displayed the same behavior as II_Ecoli by being unable to proceed through the secondary structure. However, an interesting result is that II_Salm gives rise to fragments of 21−23 nucleotides, slightly shorter than those from II_Ecoli, indicating that this protein can move closer to the double-stranded region of the substrate (Figure 2B).

E. coli RNase R is known to be capable of degrading the 16−30ds substrate to near completion, releasing a final end product of two nucleotides (*33*). In agreement with our prediction, all the RNase R-like proteins were able to degrade the 16−30ds substrate close to completion, leaving the characteristic two-nucleotide end product (Figure 2B). This confirms their ability to efficiently degrade an extensive region of double-stranded RNA.

These results show that the only member of the RNase II family found in both strains of *S. pneumoniae* analyzed has an activity similar to that of RNase R. Indeed, RNase R has been shown to be the only hydrolytic enzyme, and even the only exoribonuclease present in several organisms (*3*).

RNA Binding Ability. We were also interested in characterizing the proteins regarding their RNA binding ability. For that, the dissociation constants (K_D) were determined by surface plasmon resonance analysis (SPR) using Biacore 2000, and the data are presented in Table 3. The analysis of the results obtained showed that all the proteins studied in this work exhibit K_D values in the same range for both substrates tested [a 25-nucleotide RNA oligomer and a 30-nucleotide poly(A) RNA]. II_Ecoli presented a K_D value of 6.5 ± 0.4 nM (*11*), while R_Ecoli exhibited 2 times more affinity for the 25-nucleotide RNA

oligomer [3.2 ± 0.4 nM (Table 3)]. Such a difference was not as pronounced when the substrate analyzed was a 30-nucleotide poly(A) RNA (1.3 ± 0.4 and 1.2 ± 0.1 nM for II_Ecoli and R_Ecoli, respectively). This may be explained since this type of substrate has been described as the preferred substrate for RNase II (*53*).

The results obtained for the 25-nucleotide RNA oligomer showed that the II_Salm protein had a 2-fold reduction in the RNA affinity (6.5 ± 0.4 nM) when compared to that of the *E. coli* homologue (12.0 ± 2.0 nM) (Table 3). R_Salm was the protein that exhibited the lowest affinity for the 25-nucleotide ssRNA substrate with a K_D value of 19.7 ± 1.6 nM. With regard to the *S. pneumoniae* RNases, both proteins presented a slight reduction in their RNA binding ability, with a small increase in their K_D values when compared to R_Ecoli (16.9 ± 1.6 and 9.6 ± 0.6 nM for R_Pneumo_T4 and R_Pneumo_TIGR, respectively) (Table 3).

When the RNA binding ability was analyzed with the poly(A) substrate, the overall behavior was maintained. Contrary to what happens in *E. coli*, in *Sa. typhimurium* the II_Salm protein had a higher RNA affinity with a 2-fold reduction in the K_D value (3.7 ± 0.1 nM) when compared to that of R_Salm (7.0 ± 0.6 nM) (Table 3), suggesting that poly(A) might not be the preferred substrate of II_Salm. R_Pneumo_T4 and R_Pneumo_TIGR presented the following dissociation constants for the analysis of the poly(A) substrate: 5.7 ± 0.7 and 3.3 ± 0.2 nM, respectively. Once again, the tendency was kept among the *S. pneumoniae* proteins with R_Pneumo_TIGR being the one that exhibits the higher RNA−protein affinity of the two tested.

DISCUSSION

Some exoribonucleases have been described as being involved in the modulation of the expression of virulence in a number of pathogenic organisms (*20*, *24*, *25*). Since not much is known about RNases in *S. pneumoniae* or *Sa. typhimurium*, two widespread human pathogens, we focused our study on the biochemical characterization of the RNase II family of proteins present in these microorganisms.

In our initial analysis, we searched for homologues of the RNase II family of proteins in the genomic sequences of *Sa. typhimurium* and *S. pneumoniae* and sequenced the corresponding region of nonvirulent *S. pneumoniae* strain T4. We were able to identify two homologues of the RNase II family of proteins in *Sa. typhimurium*, while only one member of this family was found in *S. pneumoniae*.

Biochemical characterization of the identified proteins showed that one of the two hydrolytic enzymes found in *Sa. typhimurium* behaves like RNase II and the other like RNase R, which agrees with the prediction made by sequence comparison. However, in *S. pneumoniae*, the only hydrolytic enzyme present in both strains behaves like RNase R, since it is able to degrade structured RNAs and the shortest product released is two nucleotides in length.

Interestingly, our results showed that the products generated by II_Salm with the 16−30ds substrate were slightly smaller in size than those of II_Ecoli, suggesting that this protein can more closely approach the double-stranded region. A similar result had previously been reported with an RNase II mutant lacking an N-terminal CSD domain (*33*), and the explanation given to this behavior was based on the fact that the

absence of one RNA-binding domain in this protein would result in less steric hindrance, allowing the RNA substrate to move closer to the catalytic pocket. Similarly, in II_Salm, there may be a different rearrangement in the RNA binding domains that could result in a wider anchoring region. This would allow the substrate to move nearer to the catalytic cavity, even though the double-stranded moiety would impede further degradation. Another explanation could be a slight difference in their catalytic cavities, and this could account for the 88% level of amino acid identity of the RNB domains of both enzymes (Figure 1A). To gain further insight in the analysis of the results, homology-based 3D models were generated for all the proteins under study (Figure 3). The models clearly indicate that these four enzymes share a common 3D arrangement, being all the critical residues for exoribonucleolytic activity (*11*, *54*) located in equivalent spatial positions. Superimposition of the II_Ecoli crystal structure with the generated II_Salm 3D model did not reveal significant conformational changes (data not shown) that could confirm any of the hypotheses stated above. However, slight structural differences may account for the observed results. In contrast to II_Ecoli, our results indicate that poly(A) RNA may not be the preferred substrate of II_Salm. This raises the question of the role of II_Salm in digesting poly(A) tails in vivo and the consequent protection of full-length RNAs, suggesting a different RNA metabolism in *Salmonella*.

The hydrolytic enzymes from the two *S. pneumoniae* strains exhibited the same behavior with regard to the pattern of degradation of the RNA substrates studied. However, the R_Pneumo_TIGR enzyme from the virulent strain is ~50% more active than that from the nonvirulent strain. Moreover, this protein also exhibited a higher RNA affinity. These two factors can be related since a higher affinity for an RNA substrate may increase the activity of the enzyme. There is a close relation between the ability of the proteins to bind to the substrate and its processivity. In the case of exoribonucleases, the enzymes need to bind well enough to attach themselves to the RNA but not bind so strongly that they impede the translocation of the RNA. The variation between the pneumococcal enzymes might be linked with the different amino acids identified in the two enzymes (see Figure 1D). According to the 3D models, the first different amino acid between R_Pneumo_TIGR and R_Pneumo_T4 falls into the variable region before the first CSD of the enzymes, and the last is located after the S1 domain. Hence, these two amino acids most probably do not account for the observed variation in the activity and binding between the two enzymes. One of the substitutions (serine in T4, proline in TIGR4) is placed inside the CSD2 domain. This change may be related to the different binding ability displayed by the two proteins. However, the most interesting difference falls inside the RNB catalytic domain. In II_Ecoli, the active site contains four conserved aspartic acid residues. Four aspartate residues in R_Ecoli are also predicted to be involved in the coordination of the Mg^{2+} ion, which is essential for catalysis (*9*). In the active site, in the vicinity of the four conserved aspartate residues, a leucine (L285) in T4 is replaced with a phenylalanine (F285) in TIGR4. Although leucine is usually conserved in this position, the replacement with an aromatic amino acid may confer R_Pneumo_TIGR the ability to bind RNA more tightly and enhance its exoribonucleolytic activity. In fact, the RNB domain of RNase R is known to bind to RNA more tightly than the RNB domain of RNase II, and the exoribonucleolytic activity is less dependent on the
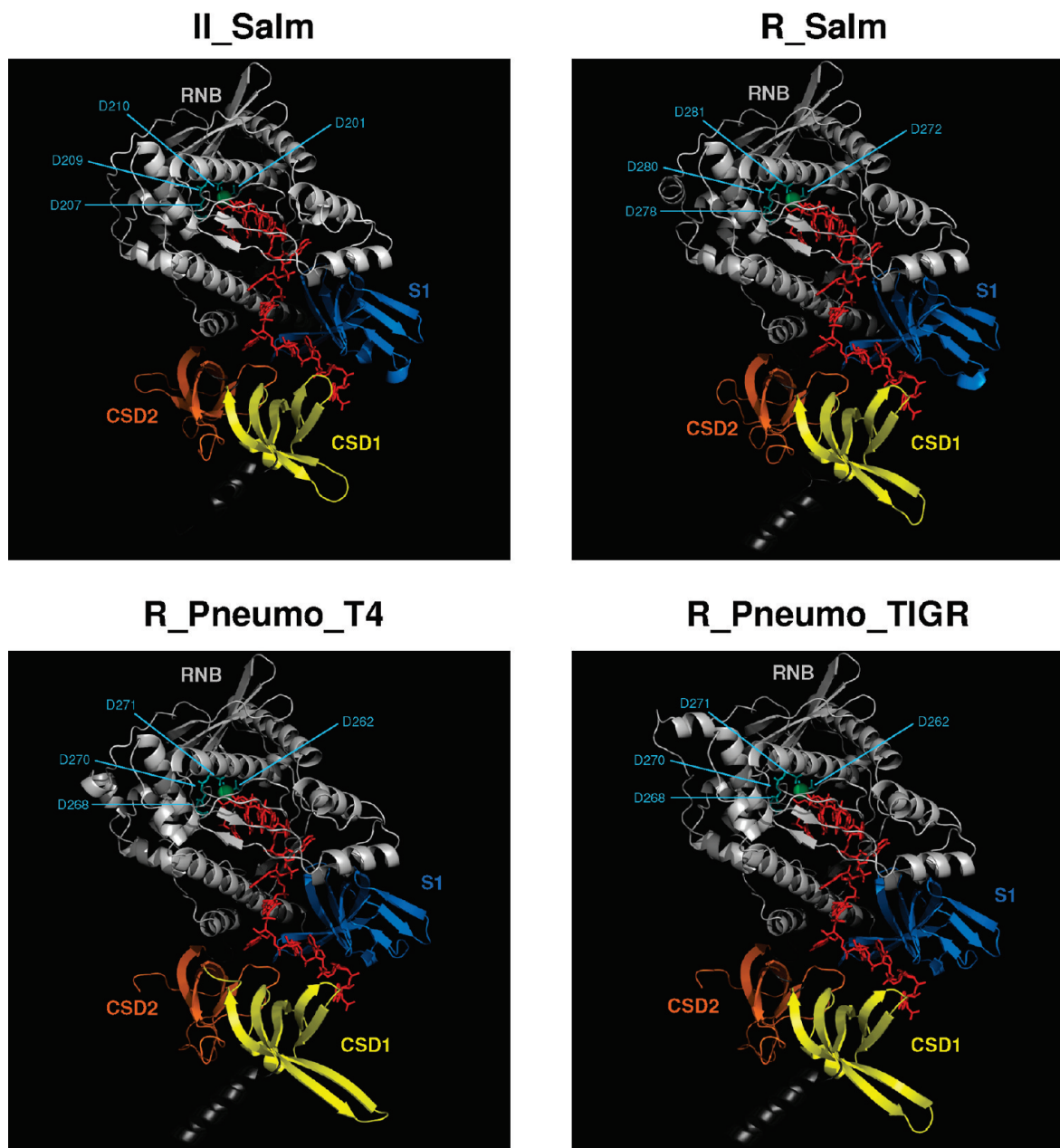
FIGURE 3: Predictive 3D models of the *E. coli* RNase II orthologues: II_Salm (amino acids 3−644), R_Salm (amino acids 65−726), R_Pneumo_T4 (amino acids 44−705), and R_Pneumo_TIGR (amino acids 44−705). A view of the cartoons from the 3D models showing domains CSD1 (yellow), CSD2 (orange), RNB (light gray), and S1 (blue) is presented. The RNA molecule (red) and the Mg^{2+} ion (green) were superimposed in all the models. The position of all equivalent residues of the catalytic site of the RNase II enzyme is indicated in all proteins. The regions excluded from the models were due to the lack of an appropriately aligned template structure.

presence of the CSDs and S1 domain (*52*, *55*). According to the analysis of the 3D models (Figure 4), although this amino acid does not seem to contact the RNA molecule directly, the spatial arrangement of the aromatic side chain of F285 may induce subtle conformational changes in the helix below that could account for the observed differences between the two enzymes. This helix corresponds to helix α8, known to contact the RNA molecule in the *E. coli* RNase II crystal structure (*9*). Thus, the substitution of this amino acid alone may be responsible for the different biochemical properties exhibited by R_Pneumo_TIGR.

This was the first time that ribonucleases of the RNase II family of *Sa. typhimurium* and *S. pneumoniae* were biochemically characterized, bringing new insights into the RNA metabolism of these two human pathogens of clinical importance. Although there are a number of genes involved in virulence, the characterization of the biochemical mode of action of proteins that might be involved in the expression of genes related to pathogenicity may be helpful for the understanding of the virulence mechanisms.
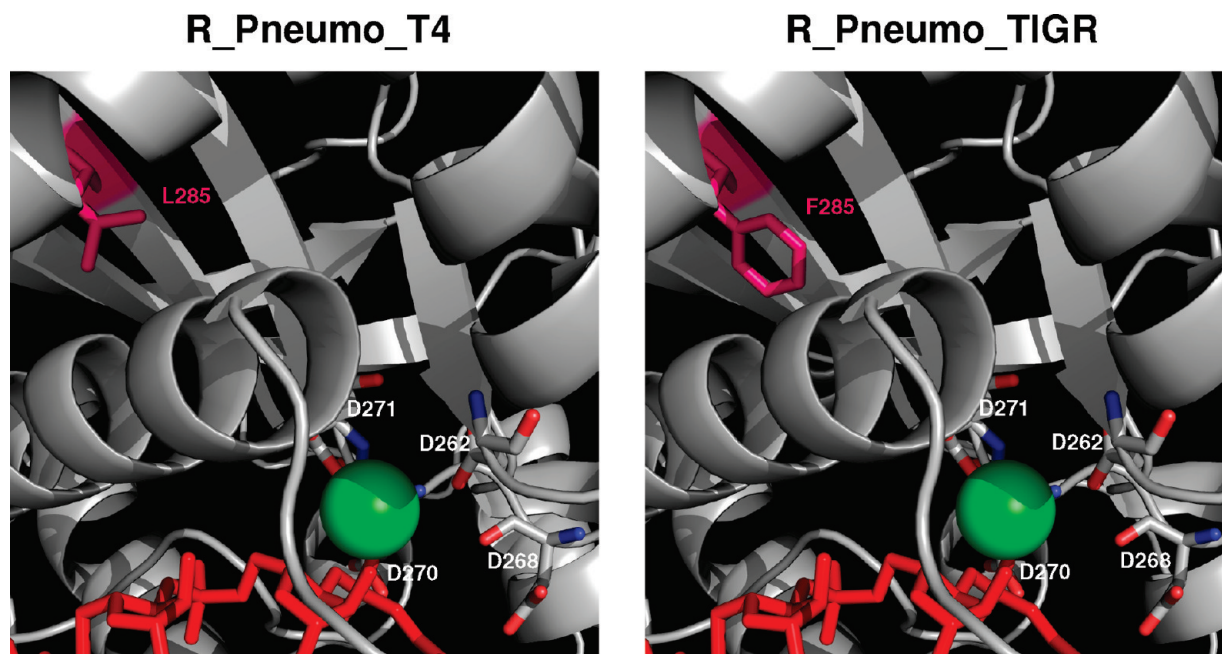
R_Pneumo_T4

R_Pneumo_TIGR

FIGURE 4: Magnified views of the proposed catalytic regions of the R_Pneumo_T4 and R_Pneumo_TIGR enzymes. The four aspartate residues involved in the coordination of the Mg^{2+} ion (green) are indicated, and the superimposed RNA molecule is colored red. L285 (pink) in R_Pneumo_T4 is replaced with F285 (pink) in R_Pneumo_TIGR.

SUPPORTING INFORMATION AVAILABLE

SDS−PAGE analysis of the purified proteins. This material is available free of charge via the Internet at http://pubs.acs.org.

REFERENCES

1. Mian, I. S. (1997) Comparative sequence analysis of ribonucleases HII, III, II, PH and D. *Nucleic Acids Res. 25*, 3187–3195.
2. Zuo, Y., and Deutscher, M. P. (2001) Survey and Summary. Exoribonuclease superfamilies: Structural analysis and phylogenetic distribution. *Nucleic Acids Res. 209*, 1017–1026.
3. Andrade, J. M., Pobre, V., Silva, I. J., Domingues, S., and Arraiano, C. M. (2009) The role of 3′-5′ exoribonucleases in RNA degradation. *Prog. Nucleic Acid Res. Mol. Biol. 85*, 187–229.
4. Deutscher, M. P., and Reuven, N. B. (1991) Enzymatic basis for hydrolytic versus phosphorolytic mRNA degradation in *Escherichia coli* and *Bacillus subtilis*. *Proc. Natl. Acad. Sci. U.S.A. 88*, 3277–3280.
5. Marujo, P. E., Hajnsdorf, E., Le Derout, J., Arraiano, C. M., and Régnier, P. (2000) RNase II removes the oligo(A) tails that destabilize the rpsO mRNA of *Escherichia coli*. *RNA 6*, 1185–1193.
6. Mohanty, B. K., and Kushner, S. R. (2000) Polynucleotide phosphorylase, RNase II and RNase E play different roles in the *in vivo* modulation of polyadenylation in *Escherichia coli*. *Mol. Microbiol. 36*, 982–994.
7. Cairrão, F., Chora, A., Zilhão, R., Carpousis, J., and Arraiano, C. M. (2001) RNase II levels change according to the growth conditions: Characterization of *gmr*, a new *Escherichia coli* gene involved in the modulation of RNase II. *Mol. Microbiol. 276*, 19172–19181.
8. Zilhão, R., Cairrão, F., Régnier, P., and Arraiano, C. M. (1996) PNPase modulates RNase II expression in *Escherichia coli*: Implications for mRNA decay and cell metabolism. *Mol. Microbiol. 20*, 1033–1042.
9. Frazão, C., McVey, C. E., Amblar, M., Barbas, A., Vonrhein, C., Arraiano, C. M., and Carrondo, M. A. (2006) Unravelling the dynamics of RNA degradation by ribonuclease II and its RNA-bound complex. *Nature 443*, 110–114.
10. Zuo, Y., Vincent, H. A., Zhang, J., Wang, Y., Deutscher, M. P., and Malhotra, A. (2006) Structural basis for processivity and single-strand specificity of RNase II. *Mol. Cell 24*, 149–156.
11. Barbas, A., Matos, R. G., Amblar, M., Lopez-Vinas, E., Gomez-Puertas, P., and Arraiano, C. M. (2008) New Insights into the Mechanism of RNA Degradation by Ribonuclease II: Identification of the residue responsible for setting the RNase II end-product. *J. Biol. Chem. 283*, 13070–13076.
12. Andrade, J. M., Cairrão, F., and Arraiano, C. M. (2006) RNase R affects gene expression in stationary phase: Regulation of *omp*A. *Mol. Microbiol. 60*, 219–228.
13. Cairrão, F., Cruz, A., Mori, H., and Arraiano, C. M. (2003) Cold shock induction of RNase R and its role in the maturation of the quality control mediator SsrA/tmRNA. *Mol. Microbiol. 50*, 1349–1360.
14. Cheng, Z. F., and Deutscher, M. P. (2003) Quality control of ribosomal RNA mediated by polynucleotide phosphorylase and RNase R. *Proc. Natl. Acad. Sci. U.S.A. 100*, 6388–6393.
15. Mahan, M. J., Slauch, J. M., and Mekalanos, J. J. (1996) Environmental regulation of virulence gene expression in *Escherichia, Salmonella and Shigella spp.* In E. coli and Salmonella: Cell and Molecular Biology , 2nd ed., pp 2803−2815, American Society for Microbiology Press, Washington, DC.
16. Li, Z., Reimers, S., Pandit, S., and Deutscher, M. P. (2002) RNA quality control: Degradation of defective transfer RNA. *EMBO J. 21*, 1132–1138.
17. Chen, C., and Deutscher, M. P. (2005) Elevation of RNase R in response to multiple stress conditions. *J. Biol. Chem. 280*, 34393–34396.
18. Charpentier, X., Faucher, S. P., Kalachikov, S., and Shuman, H. A. (2008) Loss of RNase R induces competence development in Legionella pneumophila. *J. Bacteriol. 190*, 8126–8136.
19. Purusharth, R. I., Klein, F., Sulthana, S., Jager, S., Jagannadham, M. V., Evguenieva-Hackenberg, E., Ray, M. K., and Klug, G. (2005) Exoribonuclease R interacts with endoribonuclease E and an RNA helicase in the psychrotrophic bacterium *Pseudomonas syringae* Lz4W. *J. Biol. Chem. 280*, 14572–14578.
20. Erova, T. E., Kosykh, V. G., Fadl, A. A., Sha, J., Horneman, A. J., and Chopra, A. K. (2008) Cold shock exoribonuclease R (VacB) is involved in *Aeromonas hydrophila* pathogenesis. *J. Bacteriol. 190*, 3467–3474.
21. Reva, O. N., Weinel, C., Weinel, M., Bohm, K., Stjepandic, D., Hoheisel, J. D., and Tummler, B. (2006) Functional genomics of stress response in *Pseudomonas putida* KT2440. *J. Bacteriol. 188*, 4079–4092.
22. Cheng, Z. F., and Deutscher, M. P. (2005) An important role for RNase R in mRNA decay. *Mol. Cell 17*, 313–318.
23. Cheng, Z. F., Zuo, Y., Li, Z., Rudd, K. E., and Deutscher, M. P. (1998) The *vac*B gene required for virulence in *Shigericia flexneri* and *Escherichia coli* encodes the exoribonuclease RNase R. *J. Biol. Chem. 273*, 14077–14080.
24. Tobe, T., Sasakawa, C., Okada, N., Honma, Y., and Yoshikawa, M. (1992) *vac*B, a novel chromosomal gene required for expression of virulence genes on the large plasmid of *Shigella flexneri*. *J. Bacteriol. 174*, 6359–6367.

25. Tsao, M. Y., Lin, T. L., Hsieh, P. F., and Wang, J. T. (2009) The 3′-to-5′ exoribonuclease (HP1248) of *Helicobacter pylori* regulates motility and apoptosis-inducing genes. *J. Bacteriol. 191*, 2691–2702.

26. Lalonde, M. S., Zuo, Y., Zhang, J., Gong, X., Wu, S., Malhotra, A., and Li, Z. (2007) Exoribonuclease R in *Mycoplasma genitalium* can carry out both RNA processing and degradative functions and is sensitive to RNA ribose methylation. *RNA 13*, 1957–1968.

27. Zuo, Y., and Deutscher, M. P. (2001) Exoribonuclease superfamilies: Structural analysis and phylogenetic distribution. *Nucleic Acids Res. 29*, 1017–1026.

28. Hutchison, C. A., Peterson, S. N., Gill, S. R., Cline, R. T., White, O., Fraser, C. M., Smith, H. O., and Venter, J. C. (1999) Global transposon mutagenesis and a minimal *Mycoplasma* genome. *Science 286*, 2165–2169.

29. Tomasz, A. (1999) New faces of an old pathogen: Emergence and spread of multidrug-resistant *Streptococcus pneumoniae*. *Am. J. Med. 107*, 55S–62S.

30. Hoskins, J., Alborn, W. E. Jr., Arnold, J., Blaszczak, L. C., Burgett, S., DeHoff, B. S., Estrem, S. T., Fritz, L., Fu, D. J., Fuller, W., Geringer, C., Gilmour, R., Glass, J. S., Khoja, H., Kraft, A. R., Lagace, R. E., LeBlanc, D. J., Lee, L. N., Lefkowitz, E. J., Lu, J., Matsushima, P., McAhren, S. M., McHenney, M., McLeaster, K., Mundy, C. W., Nicas, T. I., Norris, F. H., O'Gara, M., Peery, R. B., Robertson, G. T., Rockey, P., Sun, P. M., Winkler, M. E., Yang, Y., Young-Bellido, M., Zhao, G., Zook, C. A., Baltz, R. H., Jaskunas, S. R., Rosteck, P. R.Jr., Skatrud, P. L., and Glass, J. I. (2001) Genome of the bacterium *Streptococcus pneumoniae* strain R6. *J. Bacteriol. 183*, 5709–5717.

31. Taylor, R. G., Walker, D. C., and McInnes, R. R. (1993) *E. coli* host strains significantly affect the quality of small scale plasmid DNA preparations used for sequencing. *Nucleic Acids Res. 21*, 1677–1678.

32. Studier, F. W., and Moffatt, B. A. (1986) Selective expression of cloned genes directed by T7 RNA polymease. *J. Mol. Biol. 189*, 113–130.

33. Amblar, M., Barbas, A., Fialho, A. M., and Arraiano, C. M. (2006) Characterization of the Functional Domains of *Escherichia coli* RNase II. *J. Mol. Biol. 360*, 921–933.

34. Amblar, M., Barbas, A., Gomez-Puertas, P., and Arraiano, C. M. (2007) The role of the S1 domain in exoribonucleolytic activity: Substrate specificity and multimerization. *RNA 13*, 317–327.

35. Viegas, S. C., Pfeiffer, V., Sittka, A., Silva, I. J., Vogel, J., and Arraiano, C. M. (2007) Characterization of the role of ribonucleases in *Salmonella* small RNA decay. *Nucleic Acids Res. 35*, 7651–7664.

36. Arraiano, C. M., Barbas, A., and Amblar, M. (2008) Characterizing Ribonucleases *in vitro*: Examples of Synergies between Biochemical and Structural Analysis. *Methods Enzymol. 447*, 131–160.

37. Amblar, M., and Arraiano, C. M. (2005) A single mutation in *Escherichia coli* ribonuclease II inactivates the enzyme without affecting RNA binding. *FEBS J. 272*, 363–374.

38. Park, S., Myszka, D. G., Yu, M., Littler, S. J., and Laird-Offringa, I. A. (2000) HuD RNA recognition motifs play distinct roles in the formation of a stable complex with AU-rich RNA. *Mol. Cell. Biol. 20*, 4765–4772.

39. Higgins, D. G., and Sharp, P. M. (1988) CLUSTAL: A package for performing multiple sequence alignment on a microcomputer. *Gene 73*, 237–244.

40. Schmidt, H. A., Strimmer, K., Vingron, M., and von Haeseler, A. (2002) TREE-PUZZLE: Maximum likelihood phylogenetic analysis using quartets and parallel computing. *Bioinformatics 18*, 502–504.

41. Saitou, N., and Nei, M. (1987) The neighbor-joining method: A new method for reconstructing phylogenetic trees. *Mol. Biol. Evol. 4*, 406–425.

42. Felsenstein, J. (1985) Confidence limits on phylogenies: An approach using the bootstrap. *Evolution 39*, 783–791.

43. Finn, R. D., Tate, J., Mistry, J., Coggill, P. C., Sammut, S. J., Hotz, H. R., Ceric, G., Forslund, K., Eddy, S. R., Sonnhammer, E. L., and Bateman, A. (2008) The Pfam protein families database. *Nucleic Acids Res. 36*, D281–D288.

44. Kelley, L. A., and Sternberg, M. J. (2009) Protein structure prediction on the Web: A case study using the Phyre server. *Nat. Protoc. 4*, 363–371.

45. Zhang, R. G., Kim, Y., Skarina, T., Beasley, S., Laskowski, R., Arrowsmith, C., Edwards, A., Joachimiak, A., and Savchenko, A. (2002) Crystal structure of *Thermotoga maritima* 0065, a member of the IclR transcriptional factor family. *J. Biol. Chem. 277*, 19183–19190.

46. DeLano, W. L. (2002) The PyMOL Molecular Graphics System , 0.83 ed., DeLano Scientific, San Carlos, CA.

47. Ygberg, S. E., Clements, M. O., Rytkonen, A., Thompson, A., Holden, D. W., Hinton, J. C., and Rhen, M. (2006) Polynucleotide phosphorylase negatively controls spv virulence gene expression in *Salmonella enterica*. *Infect. Immun. 74*, 1243–1254.

48. Miyoshi, A., Rosinha, G. M., Camargo, I. L., Trant, C. M., Cardoso, F. C., Azevedo, V., and Oliveira, S. C. (2007) The role of the vacB gene in the pathogenesis of *Brucella abortus*. *Microbes Infect. 9*, 375–381.

49. Brennan, R. G., and Matthews, B. W. (1989) The helix-turn-helix DNA binding motif. *J. Biol. Chem. 264*, 1903–1906.

50. Liu, W., Seto, J., Sibille, E., and Toth, M. (2003) The RNA binding domain of Jerky consists of tandemly arranged helix-turn-helix/homeodomain-like motifs and binds specific sets of mRNAs. *Mol. Cell. Biol. 23*, 4083–4093.

51. Hosaka, H., Nakagawa, A., Tanaka, I., Harada, N., Sano, K., Kimura, M., Yao, M., and Wakatsuki, S. (1997) Ribosomal protein S7: A new RNA-binding motif with structural similarities to a DNA architectural factor. *Structure 5*, 1199–1208.

52. Matos, R. G., Barbas, A., and Arraiano, C. M. (2009) RNase R mutants elucidate the catalysis of structured RNA: RNA-binding domains select the RNAs targeted for degradation. *Biochem. J. 423*, 291–301.

53. Coburn, G. A., and Mackie, G. A. (1996) Overexpression, purification and properties of *Escherichia coli* ribonuclease II. *J. Biol. Chem. 271*, 1048–1053.

54. Barbas, A., Matos, R. G., Amblar, M., Lopez-Vinas, E., Gomez-Puertas, P., and Arraiano, C. M. (2009) Determination of key residues for catalysis and RNA-cleavage specificity: One mutation turns RNase II into a "super"-enzyme. *J. Biol. Chem. 284*, 20486–20498.

55. Vincent, H. A., and Deutscher, M. P. (2009) The roles of individual domains of RNase R in substrate binding and exoribonuclease activity. The nuclease domain is sufficient for digestion of structured RNA. *J. Biol. Chem. 284*, 486–494.